JOURNAL OF GEOPHYSICAL RESEARCH: ATMOSPHERES, VOL. 118, 7516–7522, doi:10.1002/jgrd.50583, 2013

Tree-ring-based snowfall record for cold arid western Himalaya, India since A.D. 1460

Ram R. Yadav[1] and Mahendra R. Bhutiyani[2]

Received 26 November 2012; revised 6 June 2013; accepted 9 June 2013; published 22 July 2013.

[1] Understanding snowfall variations in high-elevation cold arid regions of the western Himalaya is important as snowmelt water is the main source of water to meet the scores of socioeconomic needs. The ground-based observational data, though limited to the last two decades, show decreasing snowfall, raising the concern of looming water scarcity in the region. The tree-ring data of Himalayan cedar from a network of six moisture-stressed sites, where snowmelt water is the sole source of soil moisture for tree growth, were used to develop the November–April snow water equivalent (SWE) extending back to A.D. 1460. The reconstruction revealed persistent severe droughts in the 1780s followed by the 1480s and relatively lesser magnitude droughts in the 1540s–1560s, 1740s, and early twentieth century. The pluvial conditions observed in 1948–1958 and 1986–1996 stand out over any other period of such duration. The SWE reconstruction revealed large-scale spatial coherence with the corresponding month's Palmer Drought Severity Index over the western Himalayan region. Significant relationship observed between SWE reconstruction and January–March Chenab River flow revealed its potential utility in understanding water resource availability in the long-term perspective.

Citation: Yadav, R. R., and M. R. Bhutiyani (2013), Tree-ring-based snowfall record for cold arid western Himalaya, India since A.D. 1460, *J. Geophys. Res. Atmos.*, *118*, 7516–7522, doi:10.1002/jgrd.50583.

1. Introduction

[2] The incidence of droughts in cold arid regions of the western Himalaya associated with seasonal variability in winter snowfall severely affects the socioeconomic activities related to agriculture and hydroelectric power generation. The droughts of 1999–2001, widespread in southwest central Asia, seriously affected agriculture and civic water supplies [*DOA*, 2009]. The tropical Pacific Ocean sea surface temperatures (SSTs) are implicated for such regional-scale droughts [*Barlow et al*., 2002; *Hoerling and Kumar*, 2003]. However, the nonstationary relationship between drought anomalies and tropical Pacific SSTs seriously limits regional drought predictability [*Yadav*, 2011a]. The spatiotemporal characteristics and extremity of such droughts in the long-term perspective are not known due to the lack of long-term snowfall data from the western Himalaya. The ground and satellite-based snowfall records for the region, limited to the last two decades [*Kulkarni and Rathore*, 2003; *Kulkarni and Suja*, 2003; *Kulkarni et al*., 2010], do not provide a sufficient time window to assess the natural variability in snowfall in the long-term perspective.

[3] The tree-ring chronologies developed from moisture-stressed regions of the western Himalaya, to date, have been largely used to develop temperature and precipitation reconstructions [*Yadav and Park*, 2000; *Singh et al*., 2006, 2009; *Yadav*, 2011a, 2011b; *Yadav et al*., 2011]. The paucity of high-quality tree-ring data from inaccessible regions and also the short snowfall records in the western Himalaya have been largely responsible for the lack of any such attempt to reconstruct snowfall anomalies. The tree-ring-based snowfall reconstructions from elsewhere in the world are also few largely due to the paucity of long-term snowfall records [*Woodhouse*, 2003; *Timilsena and Piechota*, 2008; *Masiokas et al*., 2012; *Anderson et al*., 2012]. The present study is the first attempt in this direction to develop winter snow water equivalent (SWE) using the tree-ring chronology network of Himalayan cedar (*Cedrus deodara* (Roxb.) G. Don) from six moisture-stressed homogeneous ecological settings in Lahaul, the western Himalaya, India. Such studies are also of high transnational interest as snowfall is the major contributor to river discharge in many Himalayan Rivers, which feed the adjoining Himalayan countries.

2. Data and Methods

2.1. Tree-Ring Data

[4] Due to extreme aridity, vegetation in the study area of Lahaul, Himachal Pradesh is largely scrubby and devoid of trees. Nonetheless, scattered patches of forests with disjunctly growing trees are found in the Chenab River valley. These stray trees constitute ~1.11% of the geographical area of Lahaul region [*Forest Survey of India*, 2001].

[1]Birbal Sahni Institute of Palaeobotany, Lucknow, India.
[2]Snow Avalanche Study Establishment, Chandigarh, India.

Corresponding author: R. R. Yadav, Birbal Sahni Institute of Palaeobotany, 53 University Rd., Lucknow 226007, India. (rryadav2000@gmail.com)

2169-897X/13/10.1002/jgrd.50583

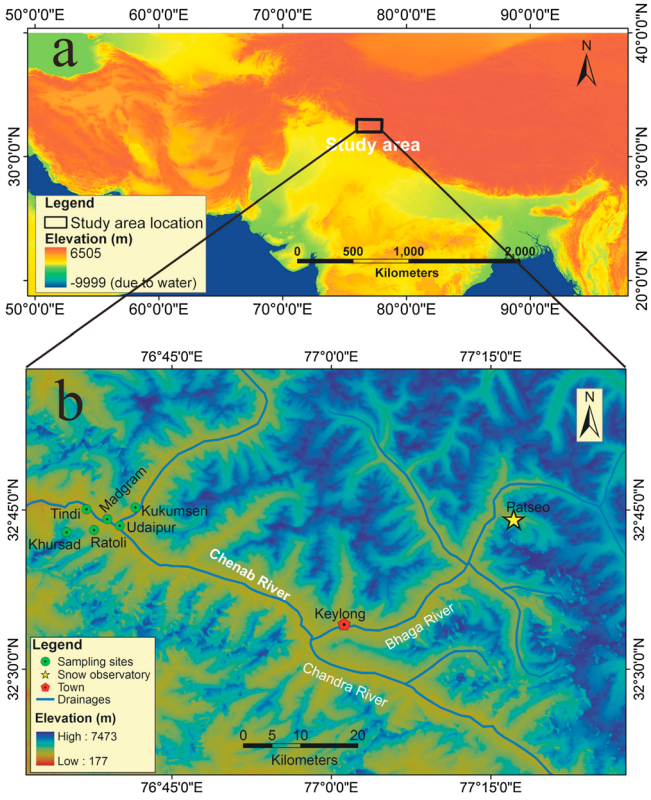

Figure 1. Location of tree-ring sampling sites and snow observing station. (a) Low-resolution map of the study area (rectangle). (b) Enlarged view of the study area showing location of sampling sites and the Patseo snow gauge station.

Such a low-density forest cover in Lahaul makes tree-ring-based climatic reconstructions difficult as old tees are hard to get here due to growing population pressure. The magnitude of human pressure in the high-elevation cold arid Lahaul region in the western Himalaya is also very high for the reason that wood provides the sole source of heating to cope with biting winter colds. However, in spite of all these factors, very old, undisturbed trees could be found over sites where tree cutting could not be possible due to steep, unapproachable rocky slopes. The increment core samples from such undisturbed, healthy trees of Himalayan cedar were collected from six sites of nearly homogeneous ecological settings in 2004 and 2008 (Figure 1). The ecological settings of sampling locations such as open, pure stands of Himalayan cedar growing on rocky slopes with thin, coarse-textured soil indicate a high likelihood of moisture stress on tree growth. Coherence in growth pattern of trees from all the sites

Table 2. Pearson Correlation in Residual Chronologies of Different Sites for the Common Period 1590–2008

Chronology	Kukumseri + Madgram	Tindi	Udaipur
Khursad + Ratoli	0.928	0.928	0.894
Kukumseri + Madgram		0.871	0.893
Tindi			0.871

indicated in COFECHA (mean r = 0.70–0.75) and ring width plots revealed a large-scale common regional climate signal affecting growth of trees. In an earlier study, 85 tree core samples having pith were pooled from all of the above six sites to develop chronology using the regional curve standardization (RCS) method [*Yadav*, 2011a]. This RCS chronology could not be calibrated with SWE data due to the existence of a weak correlation. In view of this, a larger replication of samples from respective sites was used in this study to develop independent site chronologies. In all, 161 tree cores from 131 trees collected from all the six sites were used in preparation of chronologies. To update the chronologies to the latest years, the samples from two sites collected in 2004 were pooled with the nearest respective site with similar aspect and ecological settings (Table 1). For chronology development, established dendrochronological procedures were applied [*Fritts*, 1976; *Holmes*, 1983]. Ring-width measurement series were detrended by a 100 year cubic spline with a 50% frequency response function cutoff [*Cook and Peters*, 1981]. However, before detrending, an adaptive power transformation was applied to stabilize variance in the heteroscedastic tree-ring width measurement series [*Cook and Peters*, 1997]. The growth trends were removed from the power-transformed individual measurement series by subtraction, which minimizes the end fitting-type bias as compared to the ratios. The low-order autocorrelation from detrended series was removed using autoregressive moving average modeling and the resulting residual series averaged to a mean site chronology by computing the biweight robust mean [*Cook*, 1985]. The expressed population signal (EPS) threshold of 0.85, a measure of population signal in chronologies [*Wigley et al.*, 1984], was taken as a guide to select the chronology length back to which sample replication was too small to meet this criterion. The statistics of four residual chronologies are given in Table 1. Significant correlations among chronologies for the common period 1590–2008 (Table 2) suggest common environmental forcing affecting growth dynamics of trees over different sites.

2.2. Climate of the Study Area

[5] The present study area of Lahaul in Himachal Pradesh lies between the Pir Panjal Mountains in the south and the

Table 1. Chronology (Residual) Statistics of Himalayan Cedar From Different Sites in Lahaul-Spiti, Himachal Pradesh[a]

Site No.	Site	Location	Elevation (m)	Cores/Trees	SY	Chronology With EPS >0.85	MI	MS	SD	AR1
1	Khursad[b]	32°43′N–76°37′E	2800	27/22	1217	1460–2008	0.997	0.239	0.206	−0.005
2	Ratoli[b]	32°44′N–76°37′E	3016	18/15						
3	Kukumseri[c]	32°42′N–76°41′E	2730	19/19	1187	1330–2008	0.994	0.243	0.203	−0.043
4	Madgram[c]	32°45′N–76°37′E	2710	41/25						
5	Tindi	32°52′N–76°41′E	2641	21/16	1449	1570–2008	0.999	0.251	0.211	−0.008
6	Udaipur	32°43′N–76°39′E	2640	35/34	1446	1590–2008	0.996	0.234	0.202	−0.019

[a]The details of site locations are shown in Figure 1. SY, start year of the chronology; EPS, expressed population signal; MI, mean index; MS, mean sensitivity; SD, standard deviation; AR1, first-order autocorrelation. The tree ring samples from sites with superscripts b and c respectively were merged together for chronology preparation.

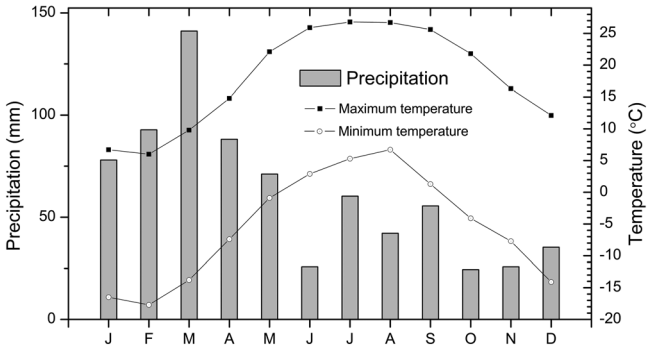

Figure 2. Monthly precipitation and mean maximum temperature and mean minimum temperature variations over Keylong in Lahaul, Himachal Pradesh.

Great Himalayan Range in the north. The region experiences extreme dry conditions due to rain shadow effect of the Pir Panjals, acting as a physical barrier to the southwest summer monsoon currents. Precipitation in the area mostly occurs during winter season largely due to eastward propagating synoptic storms [*IMD*, 2010]. The precipitation records from Keylong in Lahaul are sequentially not continuous. The continuous records barely limited to two decades show that ~72% of the annual precipitation occurs from November to April (Figure 2) [*IMD*, 2010]. Similarly, in the case of temperature, too, no observatory is maintained in the Lahaul region. Nonetheless, very old records from Keylong region [*IMD*, 2010] show that the maximum temperature ranges from 26.8°C in July to 6.0°C in February (*IMD*, 2010). The minimum temperature ranges from −17.7°C in February to 6.7°C in August (Figure 2).

2.3. SWE Data

[6] Snowfall data from the Himalayan region are few, restricted to some glacier locations for mass balance studies. In Lahaul region, frequent snow avalanches and landslides due to heavy winter snowfall cause serious loss to life and property. To understand predictability of snow avalanches, winter snowfall measurements were taken up very recently by the Snow Avalanche Study Establishment under the Ministry of Defence, Government of India. The SWE data (November–April) of Patseo (32°45′N and 77°13′E, 3800 m above sea level (asl)) from 1983–1984 to 2009–2010 (with 1989–1990 to 1991–1992 data gaps) used in present study are the only observational data available from the station close to the tree-ring sampling locations (Figure 1). The Patseo snow measurement station ~50 km from tree-ring sampling sites is located on a flat terrain surrounded by barren hills.

3. Calibration and Reconstruction of November–April SWE Data

[7] Our earlier tree-ring researches in the cold arid western Himalayan region [*Yadav*, 2011a] provided a sound basis that the growth of trees in such regions is influenced by winter precipitation. Taking this as a guide, correlation analyses between site chronologies of Himalayan cedar and November–April SWE data from Patseo were performed. The SWE data showed higher correlation with the residual version of chronologies as compared to the standard chronologies. Hence, principal component regression approach using the residual version of chronologies was adapted in the reconstruction of SWE data. To optimize the reconstruction length, a nested approach [*Meko*, 1997; *Cook et al.*, 2003] was adapted, where shorter tree-ring series are successively removed from the pool of a larger set of predictors. This involved the principal component analyses of residual version of the chronologies for the common periods of chronologies in different nest pools. A decreasing number of chronologies available for principal component analyses in subsequent nests are shown in Table 3. Given the relative shortness of SWE data (22 years), the leave-one-out cross-validation method [*Michaelsen*, 1987] was adapted for reconstruction. The linear regression models for each year were successively calibrated on the remaining 21 observations and then used to estimate the SWE value for the year omitted at each step. This resulted in 22 predicted SWE values, which were compared to the actual SWE data to compute validation statistics of model accuracy and error (Table 3) [*Fritts*, 1976]. For final reconstructions, linear regression models based on the full calibration data set (1984–2008 after omitting values for 1990, 1991, and 1992) were used to reconstruct SWE over the complete period in each nest. The first principal component (PC#1) of each nest was calibrated with full-period SWE data (i.e., 1984–2008 after omitting values for 1990, 1991, and 1992). The calibrations showed significant statistics, viz., residuals without significant first-order or higher-order autocorrelation and lack of significant trend, indicating reliability of calibration models. Three reconstructions of different lengths using a varying number of predictor chronologies in each nest were developed. The nested reconstructions were spliced together to develop the final reconstruction, which extends from A.D. 1460 to 2008. However, in order to minimize the artifact associated with the changes in variance through time due to the decreasing number of predictors, mean and standard deviation of each nested series were scaled to those of the most replicated nest (1590–2008) prior to averaging. The reconstructed mean SWE series thus developed revealed a close year-to-year similarity and significant correlation with the observed SWE series (Figure 3; $r = 0.76$, $p < 0.0001$).

Table 3. Leave-One-Out Verification Statistics of Different Nests for the Period 1984–2008 With Data Gaps of 1990–1992, R Pearson Correlation, Sign Test, Pmt (Product mean t statistics) and RE (Reduction of Error) [*Fritts*, 1976][a]

Site No.	Proxy Nests	Number of Series	R	Sign Test	Pmt	RE
1	1590–2008	4	0.59	$19^{+}/3^{-}$ (0.00086)	3.152 (0.0046)	0.342
2	1570–2008	3	0.60	$19^{+}/3^{-}$ (0.00086)	3.540 (0.0018)	0.352
3	1460–2008	2	0.60	$19^{+}/3^{-}$ (0.00086)	3.333 (0.003)	0.354

[a]p Values are given in parentheses.

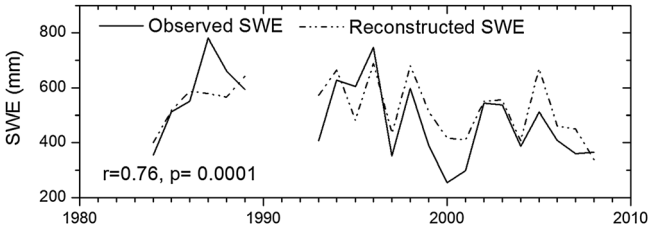

Figure 3. November–April observed and mean nest SWE reconstruction plotted to show year-to-year similarity.

[8] An independent verification of the reconstruction was performed by comparing it with precipitation data of Srinagar in Jammu and Kashmir (34°05′N and 74°50′E, 1588 m asl) in the western Himalaya where precipitation is also dominated by winter snowfall. The November–April precipitation over Srinagar showed significant correlation with the observed SWE of Patseo ($r = 0.47$, $p = 0.02$, 1984–2008, with data gaps for 1990–1992) and reconstructed SWE ($r = 0.39$, $p = 0.0001$, 1902–2008). The SWE for further cross verification was compared with the previous year (August)-current year (July) (AJ) precipitation developed for the Lahaul region using RCS chronology, though prepared using fewer replication of samples. The first differenced SWE and AJ precipitation series showed very high correlation ($r = 0.90$, $p = 0.0001$, 1461–2008). In order to understand the regional-scale features in the present SWE reconstruction, we also compared it with another tree-ring-based drought record (October–May Palmer Drought Severity Index (OM PDSI)) for the cold arid region in the western Himalaya, nearly 200 km south of the Lahaul region in Himachal Pradesh [*Yadav*, 2013]. The first differenced SWE and OM PDSI series again showed significantly high correlation ($r = 0.50$, $p < 0.0001$, 1461–2005).

[9] Additional verification to the present SWE reconstruction is again provided by the snow avalanche frequency in Lahaul region as recorded in tree rings [*Laxton and Smith*, 2008]. The variability in snowfall anomalies is associated with the magnitude and frequency of snow avalanches in hilly terrains causing serious damages to life and property [*Bhutiyani*, 1999]. The study of Himalayan cedar growth-ring features from a site close to our study area showed that the low SWEs recorded in the 1970s in our reconstruction are consistent with fewer incidences of slope failures [*Laxton and Smith*, 2008]. Similarly, high incidence of slope failures during the 1980s and 1990s and low incidence in the 2000s [*Laxton and Smith*, 2008] are consistent with high and low SWE values recorded respectively in our reconstruction. Positive (1988–1999) and negative (1999–2011) mass balances recorded in glaciers situated in the Lahaul-Spiti region [*Berthier et al.*, 2007; *Vincent et al.*, 2012] are also consistent with high and low SWE values, respectively, in our reconstruction.

4. Analyses of November–April SWE Reconstruction

[10] The November–April SWE reconstruction embedded with the smoothed version of the reconstruction using a 10 year spline curve is shown in Figure 4. The reconstruction revealed extremely low SWE values in 2008 (337.23 mm), 1782 (342.26 mm), and 1809 (343.69 mm) and high SWE in 1756 (731.26 mm), 1661 (718.46 mm), and 1730 (717.45 mm). Coupled droughts in the subsequent 2 years with severely low SWE were observed in 1537–1538, 1726–1727, 1970–1971, and 1780–1781 followed by 2000–2001. The twentieth century low and high SWE episodes recorded in our data have been also observed in winter precipitation records in the western Himalaya [*Bhutiyani et al.*, 2010]. The SWE extremes recorded in 1970 and 1971 are known to be widespread over a large part of the southwest central Asia [*Tippett et al.*, 2005]. Records available from the Lahaul region show that 1970 experienced severe drought in the region when precipitation was just 26% of the mean [*IMD*, 2010]. Similarly, droughts of 1999–2001, also widespread over the southwest central Asia, caused serious loss to agricultural production in Lahaul region [*DOA*, 2009]. To understand the longer episodes of sustained droughts and pluvial periods, the SWE was smoothed with a 7 year running mean window. Several persistent periods of anomalous SWE stand out in our reconstruction, viz., droughts in 1480–1498, 1543–1571, 1694–1708, 1739–1752, 1855–1866, 1907–1922, 1934–1944, 1968–1977, 1979–1985, and since 1998 and pluvial in 1751–1776, 1946–1963, and 1983–1999 (Figure 5). It is also of interest to note here that the decreasing snowfall in the last decades of the twentieth century also coincides with the increased warming trend in the western Himalaya. The reduced snowfall coupled with enhanced evapotranspirational water loss due to the current warming trend could aggravate the water stress in the region.

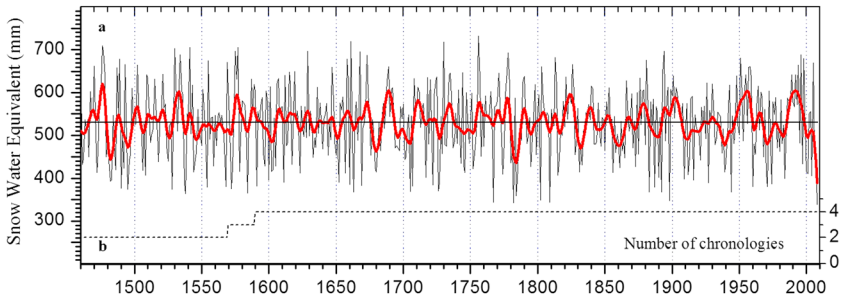

Figure 4. (a) November–April SWE (1460–2008) reconstruction plotted along with filtered version of a 10 year spline curve. (b) Number of chronologies used in reconstruction.

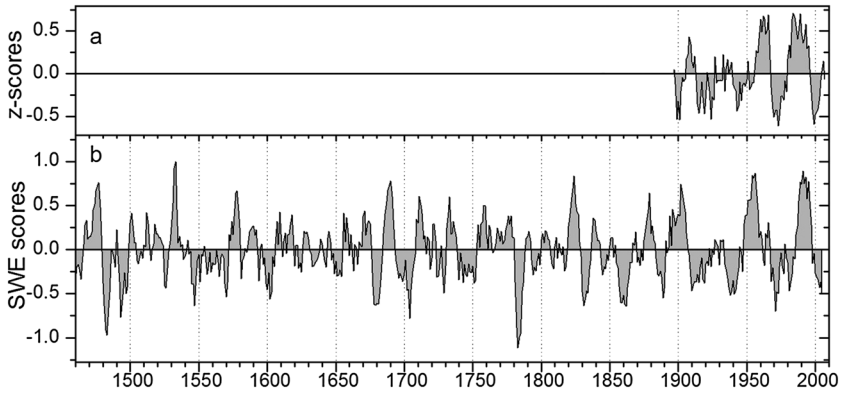

Figure 5. (a) November–April precipitation of Srinagar. (b) Reconstructed SWE. The normalized values relative to the mean of 1894–2008 were smoothed with a 7 year running average.

4.1. SWE Linkages to Regional Climate

[11] The present SWE reconstruction provides a novel opportunity to assess the relationship with the regional precipitation records. The existence of significant correlation observed between SWE and precipitation records of Srinagar (34°05′N and 74°50′E, 1588 m asl) in the western Himalaya indicated regional signatures in SWE data. The normalized November–April Srinagar precipitation and SWE after smoothing with a 7 year running mean also revealed coherent dry and pluvial periods over the twentieth century (Figure 5). Crossfield correlations using SWE data developed for the cold arid western Himalayan region and gridded PDSI (available in http://climexp.knmi.nl) [*Oldenborgh and Burgers*, 2005] were generated for 1950–2005 to understand linkages with regional droughts. The positive correlations between SWE and the corresponding months' PDSI were observed over the western Himalayan region (Figure 6a). To understand regional-scale signatures in our data, correlation fields using reconstructed SWE and June-July-August PDSI of the Monsoon Asia Drought Atlas (MADA) [*Cook et al.*, 2010] were generated (Figure 6b). The correlation fields showed distinct dipole arrangement with positive relationship over 35–45°N, 60–80°E and negative over 20–30°N, 77–85°E (Figure 6b). This relationship was further noted to be time stable over different subperiods. Such regional linkages observed in our studies revealed the potential of tree-ring data in regional climatology. However, toward this end, we are currently updating our tree-ring data from a closer network of sites in the cold arid regions of the western Himalaya, India.

4.2. Relationship Between November–April SWE and River Discharge

[12] The runoff from winter snowmelt plays an important role in driving the river flow in cold arid regions of the southwest central Asia [*Barlow and Tippett*, 2008; *Pal et al.*, 2013]. About 70% of the Chenab River basin is snow covered in March–April which is reduced to 27% in September–October [*Singh et al.*, 1997]. Such a vast difference in seasonal snow cover clearly indicates that the winter snowfall should be a major driver of river flow. In view of this, we compared our SWE reconstruction with the Chenab River flow (1970–1998) at Akhnoor (32°54′N and 74°45′E) in Jammu and Kashmir. The reconstructed SWE is significantly correlated with the Chenab River flow of January–March (Figure 7; $r = 0.57$, $p = 0.0012$) and with July (0.54, $p = 0.0025$), indicating the importance of snowmelt in the annual cycle of river flow. The dominant role of snowmelt on Satluj River flow in the winter snow-dominated region in the western Himalaya has been noted to extend up

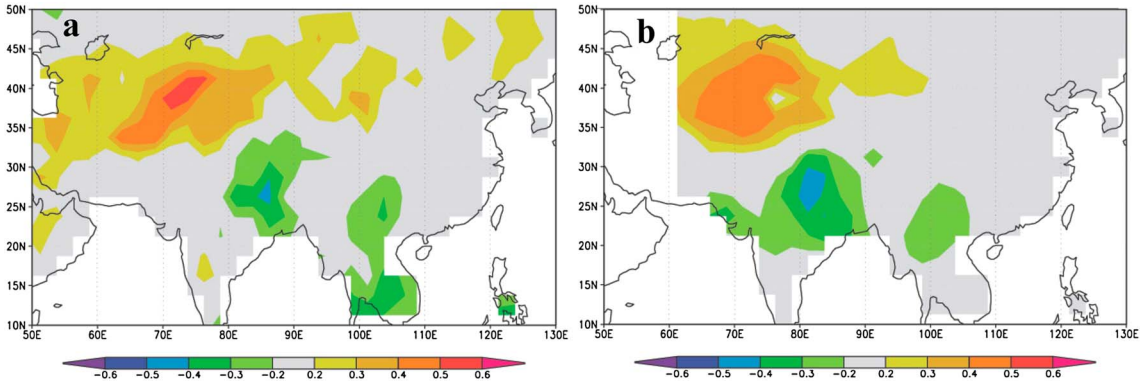

Figure 6. (a) Spatial correlation between reconstructed November–April SWE and the corresponding months' gridded PDSI data [*Dai et al.*, 2004] for 1950–2005. (b) Same as Figure 6a but between SWE and June-July-August PDSI of MADA [*Cook et al.*, 2010] for 1460–2005. Correlations were calculated after detrending the series. The pictures were generated using climate explorer program [*Oldenborgh and Burgers*, 2005].

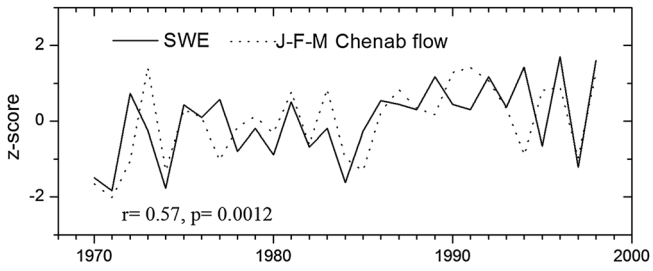

Figure 7. November–April SWE data plotted with January–March Chenab River flow at Akhnoor, Jammu and Kashmir, India. The values were normalized relative to the mean and standard deviation of the data length (1970–1998).

to the end of April [*Singh et al*., 2011]. Notwithstanding the significant correlations noted between January–March Chenab flow records at Akhnoor and SWE (Figure 7), there are clearly some mismatches in the two series. The geodesic distance between the Akhnoor gauge station and the present tree-ring study sites is ~220 km, and over such a long distance, numerous tributaries contribute to the discharge of the Chenab River. In view of this, river discharge measured at Akhnoor may not clearly reflect the Chenab flow pattern close to the tree-ring study sites. We hope that a larger tree-ring data network could prove to be a better predictor of river discharge in the Himalayan region where spatial variability in precipitation is high under the influence of dominant orographic forcing. Nonetheless, we observed that even in such a short record of river discharge data available to us, higher flow in the Chenab River in winter during 1984–1995 [*Bhutiyani et al*., 2008] corresponds well with high SWE values in our reconstruction. We compared our SWE reconstruction with the tree-ring-derived flow records of the Indus and Satluj Rivers [*Cook et al*., 2013; *Singh and Yadav*, 2013], where winter snowmelt has been implicated to be the important driver of river flow in the western Himalayan region. The 1780s with the lowest SWE in our data correspond with reduced flow in the Indus and Satluj Rivers in the western Himalaya [*Cook et al*., 2013; *Singh and Yadav*, 2013]. The other low SWE periods, viz., 1640s–1650s, 1690s, 1910s, and 1970s, are consistent with low flow in the Indus River [*Cook et al*., 2013]. The Indus flow was relatively high in the 1890s and 1980s and 1990s when high SWE was recorded in our reconstruction. The high (low) SWE values recorded in 1950s (1970s) are consistent with high (low) winter flow in the Satluj River in the western Himalaya [*Bhutiyani et al*., 2008; *Singh and Yadav*, 2013]. Such linkages in river flow and reconstructed SWE from distant regions endorse the potential of tree-ring data in regional hydrological studies in the western Himalaya. We hope a strengthened SWE reconstruction using a larger tree-ring data network from the Chenab River basin and snowfall data from more observational stations could be very useful to understand river flow dynamics in the western Himalayan cold arid regions in the long-term perspective.

5. Conclusions

[13] Ring-width chronologies of Himalayan cedar from a network of six homogeneous moisture-stressed sites in the cold arid region of Lahaul in the western Himalaya were used to develop the November–April SWE back to A.D. 1460. The SWE reconstruction with regional-scale linkages, as revealed in correlation field analyses, indicated extreme droughts in the 1780s when the Indus and Satluj Rivers flowing across the winter snowfall-dominated regions in the western Himalaya recorded extremely low discharge values. The SWE anomalies showed significant correlation with the Srinagar precipitation and gridded PDSI for wider regions in southwest central Asia. The crossfield correlations using the June–August MADA and observational PDSI revealed distinct correlations in dipole mode arrangement with positive relationship over 35–45°N, 60–80°E and negative over 20–30°N, 77–85°E. Such a strong relationship establishes the potential utility of SWE data in synoptic climatology of this region. The SWE reconstruction is further associated with the January–March and July flow of the Chenab River. However, toward the applicability of such studies in river flow studies, we need to strengthen the network of snowfall-responsive tree-ring chronologies from wider geographic regions in the prediction model. The orography-induced high snowfall variability in the Himalayan region also warrants the need to use regional mean snowfall series in the calibration model. The cross-validated snowfall reconstructions, as in the present study, involving more predictor chronologies and regional snowfall series should provide a valuable database for local water resource managers and modeling analyses intended to predict annual-to-decadal snowfall patterns which are of high relevance to society.

[14] **Acknowledgments.** R.R.Y. expresses sincere thanks to the Forest Department, Government of Himachal Pradesh for providing necessary help in the collection of tree-ring samples. The authors express sincere thanks to three anonymous reviewers, whose critical comments on the earlier version of the manuscript greatly improved the paper. The work was supported partly by ISRO-GBP and DST, New Delhi (SR/S4/ES-468/2009) research grants to R.R.Y.

References

Anderson, S., C. L. Moser, G. A. Tootle, H. D. Grissino-Mayer, J. Timilsena, and T. Piechota (2012), Snowpack reconstructions incorporating climate in the Upper Green River Basin (Wyoming), *Tree-Ring Res.*, *68*, 105–114.

Barlow, M. A., and M. K. Tippett (2008), Variability and predictability of central Asia river flows: Antecedent winter precipitation and large-scale teleconnections, *J. Clim.*, *9*, 1234–1349.

Barlow, M., H. Cullen, and B. Lyon (2002), Drought in central and southwest Asia: La Nina, the warm pool and Indian Ocean precipitation, *J. Clim.*, *15*, 697–700.

Berthier, E., Y. Arnaud, R. Kumar, S. Ahmad, P. Wagnon, and P. Chevallier (2007), Remote sensing estimates of glacier mass balances in the Himachal Pradesh (western Himalaya, India), *Remote Sens. Environ.*, *108*, 327–338.

Bhutiyani, M. R. (1999), Mass balance studies on Siachen Glacier in the Nubra Valley, Karakoram Himalaya, India, *J. Glaciol.*, *45*, 112–118.

Bhutiyani, M. R., V. S. Kale, and N. J. Pawar (2008), Changing streamflow patterns in the rivers of northwestern Himalaya: Implications of global warming in the 20th century, *Curr. Sci.*, *95*, 618–626.

Bhutiyani, M. R., V. S. Kale, and N. J. Pawar (2010), Climate change and the precipitation variations in the northwestern Himalaya: 1866-2006, *Int. J. Climatol.*, *30*, 535–548.

Cook, E. R. (1985), A time series approach to tree-ring standardization, Ph.D. thesis, University of Arizona, Tucson, 171 pp.

Cook, E. R., and K. Peters (1981), The smoothing spline: A new approach to standardizing forest interior tree-ring series for dendroclimatic studies, *Tree Ring Bull.*, *41*, 45–53.

Cook, E. R., and K. Peters (1997), Calculating unbiased tree-ring indices for the study of climatic and environmental change, *Holocene*, *7*, 361–370, doi:10.1177/095968369700700314.

Cook, E. R., P. J. Krusic, and P. D. Jones (2003), Dendroclimatic signals in long tree-ring chronologies from the Himalayas of Nepal, *Int. J. Climatol.*, *23*, 707–732.

Cook, E. R., K. J. Anchukaitis, B. M. Buckley, R. D'Arrigo, G. C. Jacoby, and W. E. Wright (2010), Asian monsoon failure and megadrought during the last millennium, *Science*, *328*, 486–489.

Cook, E. R., J. G. Palmer, M. Ahmed, C. A. Woodhouse, P. Fenwick, M. U. Zafar, M. Wahab, and N. Khan (2013), Five centuries of Upper Indus River flow from tree rings, *J. Hydrol.*, *486*, 365–375.

Dai, A., K. E. Trenberth, and T. Qian (2004), A global data set of Palmer Drought Severity Index for 1870–2002: Relationship with soil moisture and effects of surface warming, *J. Hydrometeorol.*, *5*, 1117–1130.

DOA (2009), *District Agriculture Plan: Lahaul-Spiti, H.P*, Department of Agriculture, Himachal Pradesh, vol. *VII*, pp. 103.

Forest Survey of India (2001), State of forest report 2001, Dehradun, India.

Fritts, H. C. (1976), *Tree-Rings and Climate*, Academic Press, London, pp. 567.

Hoerling, M., and A. Kumar (2003), Perfect ocean for drought, *Science*, *299*, 691–694.

Holmes, R. L. (1983), Computer-assisted quality control in tree-ring dating and measurement, *Tree-Ring Bull.*, *43*, 69–78.

IMD (2010), Climate of Himachal Pradesh, India Meteorological Department, Ministry of Earth Sciences, Govt. of India, pp. 98.

Kulkarni, A. V., and B. P. Rathore (2003), Snow cover monitoring in Baspa basin using IRS WiFS data, *Mausam*, *54*, 335–340.

Kulkarni, A. V., and A. Suja (2003), Estimation of recent glacial variations in Baspa basin using remote sensing technique, *J. Ind. Soc. Remote Sens.*, *31*, 81–90.

Kulkarni, A. V., B. P. Rathore, S. K. Singh, and Ajai (2010), Distribution of seasonal snow cover in central and western Himalaya, *Ann. Glaciol.*, *51*, 123–128.

Laxton, S. C., and D. J. Smith (2008), Dendrochronological reconstruction of snow avalanche activity in the Lahul Himalaya, northern India, *Nat. Hazards*, doi:10.1007/s11069-008-9288-5.

Masiokas, M. H., R. Villalba, D. A. Christie, E. Betman, B. H. Luckman, C. Le Quesne, M. R. Prieto, and S. Mauget (2012), Snowpack variations since AD 1150 in the Andes of Chile and Argentina (30-70S) inferred from rainfall, tree-ring and documentary records, *J. Geophys. Res.*, *117*, D05112, doi:10.1029/2011JD016748.

Meko, D. M. (1997), Dendroclimatic reconstruction with time varying subsets of tree indices, *J. Clim.*, *10*, 687–696.

Michaelsen, J. (1987), Cross-validation in statistical climate forecast models, *J. Clim. Appl. Meteorol.*, *26*, 1589–1600.

Oldenborgh, G. J., and G. Burgers (2005), Searching for decadal variations in ENSO precipitation teleconnections, *Geophys. Res. Lett.*, *32*, L15701, doi:10.1029/2005GL023110.

Pal, I., U. Lall, A. W. Robertson, M. A. Cane, and R. Bansal (2013), Diagnostics of western Himalayan Satluj River flow: Warm season (MAM/JJAS) inflow into Bhakra dam in India, *J. Hydrol.*, *478*, 132–147.

Singh, J., and R. R. Yadav (2013), Tree-ring-based seven century long flow records of Satluj River, western Himalaya, India, *Quaternary Int.*, doi:10.1016/j.quaint.2013.03.024, (in press).

Singh, P., S. K. Jain, and N. Kumar (1997), Estimation of snow and glacier-melt contribution to the Chenab River, western Himalaya, *Mt. Res. Dev.*, *17*, 49–56.

Singh, P., A. Kumar, and N. Kishore (2011), Meltwater storage and delaying characteristics of Gangotri Glacier (Indian Himalayas) during ablation season, *Hydrol. Process.*, *25*, 159–166.

Singh, J., W.-K. Park, and R. R. Yadav (2006), Tree-ring-based hydrological records for western Himalaya, India, since AD 1560, *Clim. Dyn.*, *26*, 295–303.

Singh, J., R. R. Yadav, and M. Wilmking (2009), A 694-year tree-ring based rainfall reconstruction from Himachal Pradesh, India, *Clim. Dyn.*, *33*, 1149–1158.

Timilsena, J., and T. Piechota (2008), Regionalization and reconstruction of snow water equivalent in the upper Colorado River basin, *J. Hydrol.*, *352*, 94–106.

Tippett, M. K., L. Goddard, and A. G. Barnston (2005), Statistical-dynamical seasonal forecasts of central-southwest Asian winter precipitation, *J. Clim.*, *18*, 1831–1843.

Vincent, C., et al. (2012), Mass gain of glaciers in Lahaul and Spiti region (north India) during the nineties revealed by in-situ and satellite geodetic measurements, *The Cryosphere Discuss.*, *6*, 3733–3755.

Wigley, T. M. L., K. R. Briffa, and P. D. Jones (1984), On the average value of correlated time series with applications in dendroclimatology and hydrometeorology, *Int. J. Climatol.*, *8*, 33–54.

Woodhouse, C. A. (2003), A 431-yr reconstruction of western Colorado snowpack from tree rings, *J. Clim.*, *16*, 1551–1561.

Yadav, R. R. (2011a), Tree-ring evidence of 20th century precipitation surge in monsoon shadow zone of western Himalaya, India, *J. Geophys. Res.*, *116*, D02112, doi:10.1029/2010JD014647.

Yadav, R. R. (2011b), Long-term hydroclimatic variability in monsoon shadow zone of western Himalaya, India, *Clim. Dynam.*, *36*, 1453–1462, doi:10.1007/s00382-010-0800-8.

Yadav, R. R. (2013), Tree ring-based seven-century drought records for the Western Himalaya, India, *J. Geophys. Res. Atmos.*, *118*, 4318–4325, doi:10.1029/2012JD018661.

Yadav, R. R., and W.-K. Park (2000), Precipitation reconstruction using ring width chronology of Himalayan cedar from western Himalaya: Preliminary results, *Proc. Indian Acad. Sci. Earth Planet. Sci.*, *109*, 339–345.

Yadav, R. R., A. Braeuning, and J. Singh (2011), Tree ring inferred summer temperature variations over the last millennium in western Himalaya, India, *Clim. Dynam.*, *36*, 1545–1554, doi:10.1007/s00382-009-0719-0.